Surface critical phenomena in three-dimensional percolation

Youjin Deng[1,*] and Henk W. J. Blöte[1,2]
[1]*Faculty of Applied Sciences, Delft University of Technology, P. O. Box 5046, 2600 GA Delft, The Netherlands*
[2]*Lorentz Institute, Leiden University, P. O. Box 9506, 2300 RA Leiden, The Netherlands*
(Received 19 October 2004; published 12 January 2005)

Using Monte Carlo methods and finite-size scaling, we investigate surface critical phenomena in the bond-percolation model on the simple-cubic lattice with two open surfaces in one direction. We decompose the whole lattice into percolation clusters and sample the surface and bulk dimensionless ratios Q_1 and Q_b, defined on the basis of the moments of the cluster-size distribution. These ratios are used to determine critical points. At the bulk percolation threshold p_{bc}, we determine the surface bond-occupation probability at the special transition as $p_{1c}^{(s)}=0.418\,17(2)$, and further obtain the corresponding surface thermal and magnetic exponents as $y_{t1}^{(s)}=0.5387(2)$ and $y_{h1}^{(s)}=1.8014(6)$, respectively. Next, from the pair correlation function on the surfaces, we determine $y_{h1}^{(o)}=1.0246(4)$ and $y_{h1}^{(e)}=1.25(6)$ for the ordinary and the extraordinary transition, respectively, of which the former is consistent with the existing result $y_{h1}^{(o)}=1.024(4)$. We also numerically derive the line of surface phase transitions occurring at $p_b<p_{bc}$, and determine the pertinent asymptotic values of the universal ratios Q_1 and Q_b.

DOI: 10.1103/PhysRevE.71.016117 PACS number(s): 05.50.+q, 64.60.Cn, 64.60.Fr, 75.10.Hk

I. INTRODUCTION

For a system undergoing a second-order phase transition, it is now well established [1–11] that, due to long-range correlations, surface effects on the bulk properties can be significant, and in many cases, they cannot be neglected. The surfaces can display critical phenomena that differ from the bulk critical behavior; for each bulk universality class, different surface universality classes can exist.

Because our knowledge of such surface critical phenomena in percolation problems is limited, we first review the Ising model with nearest-neighbor interactions on a three-dimensional lattice with periodic and free boundary conditions in the xy plane and along the z direction, respectively. In other words, for a finite system with linear size L, there are two open surfaces at $z=1$ and $z=L$. The interaction strengths K_1 on the surfaces can assume values different from K in the bulk. The Hamiltonian of this Ising model can then be written into two parts: a bulk term proportional to the volume of the system and a surface term proportional to the surface areas, i.e.,

$$\mathcal{H}/k_{\mathrm{B}}T = -K\sum_{\langle ij\rangle}{}^{(\mathrm{b})}s_i s_j - H\sum_{k}{}^{(\mathrm{b})}s_k - K_1\sum_{\langle lm\rangle}{}^{(\mathrm{s})}s_l s_m - H_1\sum_{n}{}^{(\mathrm{s})}s_n \quad (s=\pm 1), \tag{1}$$

where the first two sums account for the bulk and the last two sums involve the spins on the open surfaces. In the absence of bulk and surface magnetic fields H and H_1, the phase diagram of the model (1) is sketched in Fig. 1 for the case $K>0$. When the bulk temperature $1/K$ is lowered, the bulk undergoes a second-order transition at $K=K_c$ between the paramagnetic and the ferromagnetic states, denoted as BP and BF in Fig. 1, respectively. When the surface coupling K_1 is varied, the local behavior on and near the surfaces can be significantly modified. For instance, for a paramagnetic bulk $K<K_c$, the surfaces can behave as an antiferromagnet (SAF), a ferromagnet (SF), and a paramagnet (SP), depending on the sign and the strength of K_1. The corresponding phase transitions occurring on the surfaces are referred to as the "surface transitions" [1], and they are represented by the solid curved lines in Fig. 1. Due to the absence of long-ranged bulk correlations, these surface transitions display the critical behavior of the two-dimensional (2D) Ising model with anti- or ferromagnetic couplings, $K_1<0$ or $K_1>0$, respectively. Therefore, the corresponding thermal and magnetic exponents are $y_t=1$ and $y_h=15/8$ [12], respectively. For

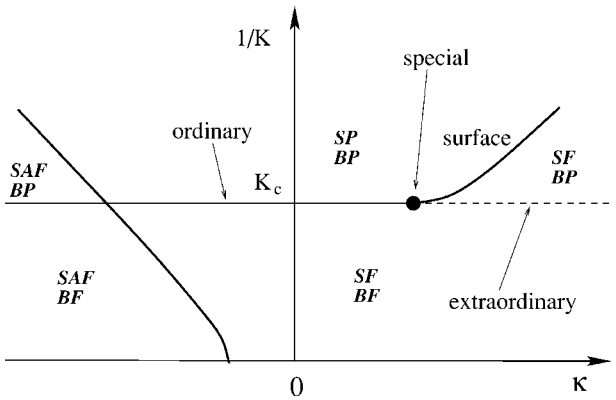

FIG. 1. Schematic phase diagram for the three-dimensional Ising model, in terms of ferromagnetic bulk couplings K and the ratio $\kappa=K_1/K$ of the surface over the bulk couplings. The bulk transition occurs at $K=K_c$. The bulk phases are denoted as BF for the ferromagnet and BP for the paramagnet. The surface phases are labeled as SF, SP, and SAF for the ferro-, para-, and antiferromagnet, respectively.

*Present address: Laboratory for Materials Science, Delft University of Technology, Rotterdamseweg 137, 2628 AL Delft, The Netherlands.

surface couplings $K_1<0$, the phase boundaries for the bulk and surface transitions cross at a decoupled critical point because of the different signs of K and K_1. We shall denote this decoupled point as $(K_c,K_{1c}^{(a)})$, and at this point there is no indication of any change in the surface universality class [4]. However, the surface critical line for $K_1>0$ terminates at the bulk criticality in a "special" critical point $(K_c,K_{1c}^{(s)})$. At this point, both the surface and the bulk correlation lengths are divergent. Thus, the point $(K_c,K_{1c}^{(s)})$ acts as a multicritical point, and the phase transition is referred to as the "special transition." When K is varied, while the surface coupling is in the range $K_{1c}^{(a)}<K_1<K_{1c}^{(s)}$, the surfaces and the bulk simultaneously undergo a phase transition at $K=K_c$. In this case, the critical correlations on the surfaces arise from the diverging bulk correlation length, and the phase transition is named the "ordinary transition." For larger couplings $K_1>K_{1c}^{(s)}$, however, the bulk transition at $K=K_c$ has to occur in the presence of spontaneous long-ranged surface order, because the surfaces become ferromagnetic at a smaller coupling $K<K_c$, and the transition is referred to as the "extraordinary transition." Thus, different universality classes apply to the surface transitions of the three-dimensional Ising model (1).

We mention that, although the local behavior near and at the surfaces can be modified by the variation of surface parameters and the decay of the surface effects into the bulk can be long ranged, the bulk properties of the system (1) are not affected. Naturally, besides the bulk thermal and magnetic exponents y_t and y_h, additional surface critical exponents are needed to describe the scaling behavior of the above phase transitions on the surfaces. To illustrate this point, one writes the total free energy F of the system (1) as the sum of a bulk and a surface term [1,10]

$$F = f_b V + f_1 S. \tag{2}$$

For a finite system with linear size L, the volume and the surface areas are $V=L^d$ and $S=2L^{d-1}$, respectively, with $d=3$ the spatial dimensionality. The prefactor 2 counts the number of the surfaces. The finite-size scaling of the bulk and the surface free energy density, f_b and f_s, can then be expressed as

$$f_b(t,h,L) = L^{-d} f_{bs}(tL^{y_t},hL^{y_h}) + f_{ba}(t,h) \tag{3}$$

and

$$f_1(t,h,t_1,h_1,L) = L^{-(d-1)} f_{1s}(tL^{y_t},hL^{y_h},t_1L^{y_{t1}},h_1L^{y_{h1}}) + f_{1a}(t,h,t_1,h_1). \tag{4}$$

The functions f_{bs} and f_{ba} are the singular and the analytical parts of f_b, respectively, and f_{1s} and f_{1a} similarly apply to the surface free-energy density f_1. The bulk thermal and magnetic scaling fields are represented by t and h, respectively, and the surface scaling fields by t_1 and h_1, with exponents denoted as y_{t1} and y_{h1} respectively. The finite-size scaling behavior of the surface quantities is obtained by differentiating Eq. (4) with respect to appropriate scaling fields. For the ordinary and the extraordinary transitions, the surface thermal field t_1 is irrelevant ($y_{t1}<0$) and the magnetic scaling field h_1 is relevant ($y_{h1}>0$); both t_1 and h_1 are relevant at the special transition $(K_c,K_{1c}^{(s)})$.

In three dimensions, exact information about critical behavior is scarce, and determinations of transition points and the corresponding critical exponents have to rely on approximations of various kinds. These include mean-field theory, series expansions, renormalization group theory, Monte Carlo simulations, etc. The bulk critical point of the Ising model (1) on the simple-cubic lattice has been determined as $K_c=0.221\,654\,55(3)$ [13]. There is also some consensus [13] that the values of the bulk thermal and magnetic exponents y_t and y_h are about 1.586 and 2.482, respectively, with differences only in the last decimal place. Further, the mean-field analysis and the Gaussian fixed point of the ϕ^4 theory yield [1,14] the exact values of the standard magnetic index β_1 as $\beta_1^{(o)}=1$, $\beta_1^{(s)}=1/2$, and $\beta_1^{(e)}=1$ for the ordinary, special, and extraordinary surface transitions, respectively. The index β_1 describes the asymptotic scaling behavior of the surface magnetization m_1 as a function of the bulk thermal field t, i.e., $m_1 \propto t^{\beta_1}$, such that it is related to the renormalization exponents as $\beta_1=(d-1-y_{h1})/y_t$. The mean-field analysis [1,14] also gives the crossover exponent at the special transition as $\Phi^{(s)}=y_{t1}/y_t=1/2$. From a simple scaling argument, it was shown [15] that, independent of the spatial dimensionality d, the surface thermal exponent at the ordinary transitions is $y_{t1}^{(o)}=-1$. Many numerical results have also been obtained. On the simple-cubic lattice, the special transition of the model (1) was located [5,16] at $\kappa_c=K_{1c}^{(s)}/K_c=1.5004(20)$; the surface exponents are determined as $y_{h1}^{(o)}=0.737(5)$ [6,9], $y_{t1}^{(s)}=0.94(6)$, and $y_{h1}^{(s)}=1.62(2)$ [5,16]. These results, together with the aforementioned bulk exponents, yield the critical indices as $\beta_1^{(o)}=0.796(5)$, $\beta_1^{(s)}=0.24(1)$, and $\Phi^{(s)}=0.59(3)$. As generally expected for systems below the upper critical dimensionality, which is 4 for Ising systems, these values differ significantly from the mean-field predictions.

Beside the Ising model, the right-hand-side part ($\kappa>0$) of the phase diagram in Fig. 1 applies to a number of other three-dimensional systems, including the $O(n)$ model with $n\leqslant 2$ and the percolation model. The XY model is a marginal case of the $O(n)$ model with $n=2$ in the sense that the two-dimensional surfaces display a Kosterlitz-Thouless-like transition for $K<K_c$ [17,18]. At the ordinary phase transitions, the surface magnetic exponent was numerically determined as $y_{h1}^{(o)}=0.790(15)$ [6]. In the context of percolation theory, the mean-field analysis [14,19] yields the critical indices $\beta_1^{(o)}=3/2$ and $\beta_1^{(s)}=1$, and the crossover exponent $\Phi^{(s)}=1/2$. Naturally, these predictions are expected to be correct only at or above the upper critical dimensionality of percolation problems, which is equal to 6. In three dimensions, a number of Monte Carlo investigations also exists [9,20,21]. The surface magnetic exponent at the ordinary phase transitions was determined as $y_{h1}^{(o)}=1.030(6)$ [21] and $y_{h1}^{(o)}=1.024(4)$ [9]. The latter result was obtained from predictions of conformal invariance combined with simulations of the anisotropic limit of the bond-percolation model on a spherocylinder. However, as far as we know, a systematic study of surface critical properties as a function of the bulk and surface parameters is

still absent. In particular, numerical estimations of the critical exponents, $y_{t1}^{(s)}$, $y_{h1}^{(s)}$, and $y_{h1}^{(e)}$, have not been reported. For this reason we conduct further explorations.

The outline of the present paper is as follows. Section II briefly reviews the definitions of the bond-percolation model and of the sampled quantities. In Sec. III, Monte Carlo data are analyzed and the results are presented for the ordinary, the special, and the extraordinary transitions, and for the line of surface phase transitions. A brief discussion is given in Sec. IV.

II. MODEL AND SAMPLED QUANTITIES

Since their original introduction in 1957 [22], percolation problems have been of great research interest to physicists and mathematicians [23], and a variety of applications [24] has been reported. In the field of critical phenomena, the percolation theory provides a simple picture and a fascinating illustration of many important concepts in terms of geometric properties. In fact, the percolation, together with the Ising model, has become an important testing ground for various methods and approaches; frequently, they are used for tutorial purposes [25].

A simple example of a percolation problem is provided by the following bond-percolation model on a regular lattice. Between each pair of nearest-neighbor sites, a bond is occupied or empty with probabilities p and $1-p$, respectively. Two sites connected through a chain of occupied bonds are said to percolate, i.e., to be in the same cluster. Then, various questions can be asked concerning the distribution of cluster sizes, the fractal dimension of the clusters, etc. It is fascinating that the bond-percolation model can be generalized to an infinite range of universality classes, namely, the random-cluster representation of the q-state Potts model [26]. The pertinent clusters are referred to as the Kasteleyn-Fortuin clusters [27]. For $q \to 1$ the random-cluster model reduces to the percolation model. As a result, much of the knowledge that has been gathered for the Potts model is directly applicable to the percolation model. For instance, the fractal dimension of percolation clusters can be identified as the magnetic scaling dimension of the $q \to 1$ Potts model. In two dimensions, the bulk thermal and magnetic exponents are [26] $y_t = 3/4$ and $y_h = 91/48$, respectively. In three dimensions, the exact values of y_t and y_h are unknown yet, but they have been numerically determined [28–30] as $y_t = 1.141(5)$ and $y_h = 2.523(4)$, respectively.

In the present work, we also chose the bond-percolation model on the simple-cubic lattice with periodic boundary conditions in the xy plane and open boundary conditions in the z direction. Again, we allow for different values of the surface and bulk bond-occupation probabilities which are denoted p_1 and p_b. Further, we make use of the existing estimate of the bulk percolation threshold $p_b = p_{bc} = 0.248\,821\,6(5)$ [28], whose precision is sufficient for the present investigation. Just as in the well-known Swendsen-Wang algorithm [31] for the Potts model, we decompose the lattice into clusters according to the bulk and surface probabilities, p_b and p_1. The size of a cluster is defined as the total number of lattice sites in that cluster. In addition, we count the number of sites in each cluster which lie on a surface. Thus, for each cluster three numbers are stored in computer memory, which are denoted n_{ib}, $n_{i1}(z=1)$, and $n_{i1}(z=L)$, where i is the cluster number. We refer to n_{ib} and n_{i1} as the bulk and the surface cluster size, respectively. On this basis, we sampled the moments of the cluster sizes as

$$l_{21} = \frac{1}{2S^2} \sum_i \{[n_{i1}(z=1)]^2 + [n_{i1}(z=L)]^2\} \quad \text{and}$$

$$l_{2b} = \frac{1}{V^2} \sum_i n_{ib}^2, \tag{5}$$

and

$$l_{41} = \frac{1}{2S^2} \sum_i \{[n_{i1}(z=1)]^4 + [n_{i1}(z=L)]^4\} \quad \text{and}$$

$$l_{4b} = \frac{1}{V^4} \sum_i n_{ib}^4, \tag{6}$$

where $S = L^2$ and $V = L^3$ are the area of one surface and the volume of the system, respectively. At the bulk percolation threshold p_{bc}, the scaling behavior of the bulk quantities l_{2b} and l_{4b} in Eqs. (5) and (6) is described by the bulk magnetic exponent y_h. Analogously, the surface critical quantities l_{21} and l_{41} are governed by the surface magnetic exponent y_{h1}, which assumes different values in different surface universality classes.

In Monte Carlo studies of phase transitions, certain dimensionless ratios [32] are known to be very helpful, particularly in the determinations of critical points. Thus, on the basis of the quantities defined in Eqs. (5) and (6), we sampled the surface and bulk ratios defined as

$$Q_1 = \langle l_{21} \rangle^2 / (3\langle l_{21}^2 \rangle - 2\langle l_{4s} \rangle) \quad \text{and}$$

$$Q_b = \langle l_{2b} \rangle^2 / (3\langle l_{2b}^2 \rangle - 2\langle l_{4b} \rangle). \tag{7}$$

The large-L asymptotic values of these ratios at criticality are universal. We mention that other definitions of universal ratios are possible, e.g., one can have $Q_b' = \langle l_{2b} \rangle^2 / \langle l_{4b} \rangle$. The particular choice of the denominators in Eq. (7) is due to the following reasons, as given in the language of the bulk ratio Q_b. First, for the limiting case $p_b \to 0$, most clusters contain only a few sites, and the distribution of the cluster sizes becomes Gaussian-like for $L \to \infty$. In this case, the quantities l_{2b} in Eq. (5) and l_{4b} in Eq. (6) are of the order $1/V$ and $1/V^3$, respectively, so that the asymptotic value approaches $Q_b(L \to \infty) = 1/3$, which correctly reflects the normal distribution. In the other limit $p_b \to 1$, a single cluster occupies a nonzero fraction of the lattice, so that one simply has $Q_b(p_b \to 1) = 1$. Second, it can be shown that, in the case of the Ising model, the quantities l_{2b} and l_{2b} in Eq. (6) are exactly related to the moments of the magnetization m as

$$\langle m_b^2 \rangle = \langle l_{2b} \rangle \quad \text{and} \quad \langle m_b^4 \rangle = 3\langle l_{2b}^2 \rangle - 2\langle l_{4b} \rangle. \tag{8}$$

Thus, the ratio Q_b in Eq. (5) is just the magnetic amplitude ratio $Q = \langle m_b^2 \rangle^2 / \langle m_b^4 \rangle$, which has been used extensively.

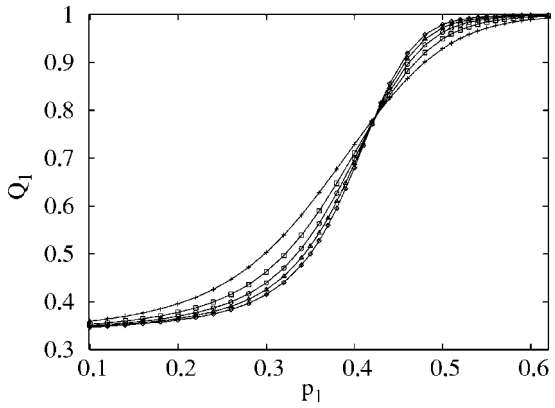

FIG. 2. Surface ratio Q_1 of the 3D bond-percolation model at bulk criticality p_{bc} vs the surface bond probability p_1. The data points +, □, ○, △, and ◇ represent system sizes $L=8$, 12, 16, 20, and 24, respectively.

In the percolation theory, quantities known as the mean cluster sizes are of some interest [23]. These quantities can be defined on the basis of n_{ib} and n_{i1} as

$$\chi_1 = \frac{1}{2S}\sum_i{}''\{[n_{is}(z=1)]^2 + [n_{is}(z=L)]^2\} \quad \text{and}$$

$$\chi_b = \frac{1}{V}\sum_i{}' n_{ib}^2, \tag{9}$$

where the latter sum excludes the largest cluster in the bulk, and the former sum excludes the largest cluster on each surface. Just like the susceptibility at a thermodynamic phase transition, the quantities χ_1 and χ_b display a peak at criticality.

We also determined the pair correlation function $g(r)$, defined as the probability that two points at a distance r lie in the same cluster. For this purpose, a number $c_{x,y,z}$ is stored for each site (x,y,z). This number is the number of the cluster to which site (x,y,z) belongs. Therefore, two sites with the same value of $c_{x,y,z}$ belong to the same cluster. On this basis, we sampled pair correlations on the surfaces at $z=1$ and $z=L$ as

$$g_{11}(r=L/2) = \frac{1}{2L^2}\sum_{x,y=1}^{L} \langle \delta_{c(x,y,1),c(x,y+r,1)} + \delta_{c(x,y,L),c(x,y+r,L)} \rangle \tag{10}$$

and

$$g_{12}(r=L) = \frac{1}{L^2}\sum_{x,y=1}^{L} \langle \delta_{c(x,y,1),c(x,y,L)} \rangle. \tag{11}$$

At criticality, the scaling behavior of $g_{11}(L)$ and $g_{12}(L)$ as a function of system size L is described by a power law; the corresponding exponent is $-2X_{h1}$, where $X_{h1}=2-y_{h1}$ is the surface magnetic scaling dimension. We further remark that the quantity $L^2\langle l_{21}\rangle$ in Eq. (5) can be obtained by integration of $g_{11}(r)$ over the surfaces.

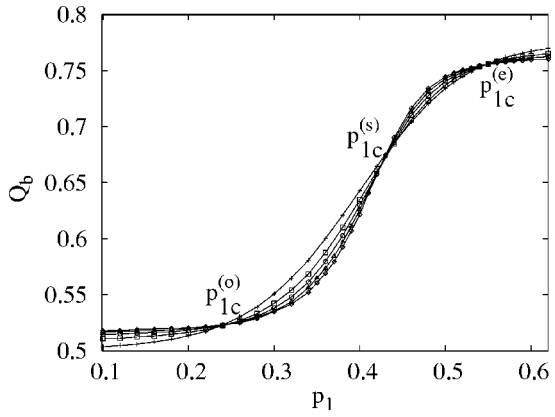

FIG. 3. Bulk ratio Q_b at bulk criticality p_{bc} vs p_1. The data points +, □, ○, △, and ◇ represent system sizes $L=8$, 12, 16, 20, and 24, respectively.

III. RESULTS

We simulated the bond-percolation model at the bulk percolation threshold $p_b=p_{bc}=0.248\,821\,6(5)$ [28]. For an illustration of the surface critical properties as a function of p_1, we took p_1 in the range $0.1\leqslant p_1\leqslant 0.62$ and the system size as $L=8$, 12, 16, and 24. The sampled quantities include the surface and the bulk ratio Q_1 and Q_b, and the surface mean cluster size χ_1. The Q_1, Q_b, and χ_1 data are shown in Figs. 2–4, respectively. These data indicate the existence of the special phase transition at about $p_{1c}^{(s)}\simeq 0.42$. The finite-size behavior of χ_1 in Fig. 4 appears to be rather asymmetric with respect to the location of the special transition at $p_{1c}^{(s)}$. At the extraordinary transitions $p_1>p_{1c}^{(s)}$, χ_1 converges rapidly to a constant as L increases. This is due to the fact that the clusters, with the exception of the largest one, are limited in size. In contrast, at the ordinary phase transitions $p_1<p_{1c}^{(s)}$, χ_1 increases significantly as a function of L. This indicates that the surfaces maintain strong critical correlations at the ordinary transition. On the other hand, the asymptotic value $Q_{1c}^{(o)}$, as shown in Fig. 2, is close the Gaussian value 1/3. This indicates that the surface critical singularities at the ordinary transition are much weaker than those at the special transition.

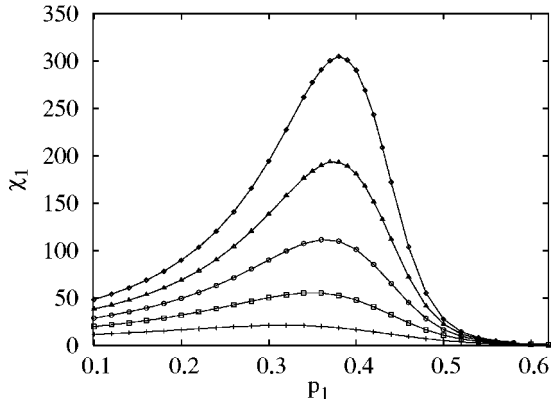

FIG. 4. Surface mean cluster size χ_1 at bulk criticality p_{bc}, vs p_1. The data points +, □, ○, △, and ◇ represent system sizes $L=8$, 12, 16, 20, and 24, respectively.

As shown in Fig. 3, the Q_b data for different system sizes display three clear intersections. These intersections correspond with the fixed points for the ordinary, the special, and the extraordinary transition, which are denoted as $p_{1c}^{(o)}$, $p_{1c}^{(s)}$, and $p_{1c}^{(e)}$, respectively. As expected, it follows from Fig. 3 that, along the p_1 direction, $p_{1c}^{(o)}$ and $p_{1c}^{(e)}$ are stable while $p_{1c}^{(s)}$ is unstable.

A. Special transition

As indicated by Figs. 2–4 the special transition occurs at $p_{1c}^{(s)} \approx 0.42$. We thus performed extensive simulations in the range $0.4 \leqslant p_1 \leqslant 0.44$ at the bulk percolation threshold p_{bc}. The sampled quantities include the surface ratio Q_1, and the surface correlation functions g_{11} and g_{12}, etc. The system sizes were chosen as 15 values in the range $6 \leqslant L \leqslant 120$. About 2.6×10^9 samples were taken for system sizes in the range $L \leqslant 20$, and 4.0×10^8 for $L > 20$. In order to save computer time, the actual simulations did not decompose the whole lattice. Instead, a Monte Carlo step was finished as soon as the two surfaces were completely divided into clusters. This does not affect the surface quantities such as l_{21} and Q_1, but the sampling of the bulk quantities such as l_{2b} and Q_b becomes incomplete. Part of the Q_1 data are shown in Fig. 5, of which the clean intersection indicates that finite-size corrections are not very important in the ratio Q_1. Near the special critical point $p_{1c}^{(s)}$, we fitted the Q_1 data by

$$Q_1(p_1,L) = Q_{1c}^{(s)} + \sum_{k=1}^{4} a_k (p_1 - p_{1c}^{(s)})^k L^{k y_{t1}^{(s)}} + \sum_{l=1}^{4} b_l L^{y_l} + c(p_1 - p_{1c}^{(s)}) L^{y_{t1}^{(s)} + y_i} + n(p_1 - p_{1c}^{(s)})^2 L^{y_{t1}^{(s)}} + r_0 L^{y_a} + r_1 (p_1 - p_{1c}^{(s)}) L^{y_a} + r_2 (p_1 - p_{1c}^{(s)})^2 L^{y_a} + r_3 (p_1 - p_{1c}^{(s)})^3 L^{y_a}, \tag{12}$$

where the terms with amplitude b_l account for various finite-size corrections. We fixed the exponent $y_1 = y_i = -1.14(15)$ [28–30], the exponent of the leading irrelevant scaling field in the three-dimensional percolation model. In principle, additional irrelevant scaling fields can be induced by the open surfaces, so that we set $y_2 = y_{i1}$ as an unknown exponent. In order to reduce the residual χ^2 without discarding data for many small system sizes, we have included further finite-size corrections with integer powers $y_3 = -2$ and $y_4 = -3$. The term with coefficient n reflects the nonlinear dependence of the scaling field on p_1, and the one with c describes the "mixed" effect of the surface thermal field and the irrelevant field. The terms with amplitudes r_0, r_1, r_2, and r_3 arise from the analytical part of the free energy, and the exponent y_a is equal to $2 - 2y_{h1}^{(s)}$. As determined later, the surface magnetic exponent at the special transition is about $y_{h1}^{(s)} = 1.8014(6)$, so that we fixed the exponent $y_a = -1.6028$. We obtain $p_{1c}^{(s)} = 0.418\,17(2)$, $Q_{1c}^{(s)} = 0.7629(2)$, $y_{t1}^{(s)} = 0.5387(2)$, and $yi1 = -2.4(20)$, where the error margins are quoted as two standard statistical deviations. The irrelevant exponent y_{i1} is not well determined, in the sense that the magnitude of the estimated error is almost as large as the exponent y_{i1} itself. We indeed found that the residuals and the results

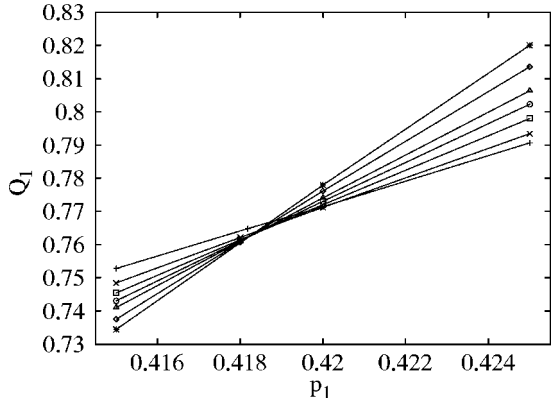

FIG. 5. Surface ratio Q_1 at bulk criticality p_{bc} in the range $0.415 \leqslant p_1 \leqslant 0.425$. The data points $+$, $\times$, $\square$, $\bigcirc$, $\triangle$, $\diamond$, and $*$ represent system sizes $L = 16$, 24, 32, 40, 48, 64, and 80, respectively.

of the fits do not significantly depend on the presence or absence of the terms with b_2.

In order to determine the surface magnetic exponent $y_{h1}^{(s)}$, we fitted the l_{21} data by

$$l_{21}(p_1,L) = L^{2y_{h1}^{(s)}-4} \Bigg(a_0 + \sum_{k=1}^{4} a_k (p_1 - p_{1c}^{(s)})^k L^{k y_{t1}^{(s)}} + b_1 L^{y_i} + b_2 L^{y_{i1}} + b_3 L^{y_3} + b_4 L^{y_4} + c(p_1 - p_{1c}^{(s)}) L^{y_{t1}^{(s)} + y_i} + n(p_1 - p_{1c}^{(s)})^2 L^{y_{t1}^{(s)}} + r_0 L^{y_a} + r_1 (p_1 - p_{1c}^{(s)}) L^{y_a} + r_2 (p_1 - p_{1c}^{(s)})^2 L^{y_a} + r_3 (p_1 - p_{1c}^{(s)})^3 L^{y_a} + c_{21}(p_1 - p_{1c}^{(s)}) L^{y_{t1}^{(s)} + y_{i1}} + c_{22}(p_1 - p_{1c}^{(s)})^2 L^{2y_{t1}^{(s)} + y_{i1}} \Bigg). \tag{13}$$

Again, the correction exponents were taken as $y_i = -1.14(15)$ [28–30], $y_3 = -2$, and $y_4 = -3$. In comparison with Eq. (12), we have included in Eq. (13) the "mixed" effect of the surface thermal field and the irrelevant field with the unknown exponent y_{i1}, as described by the terms with c_{21}

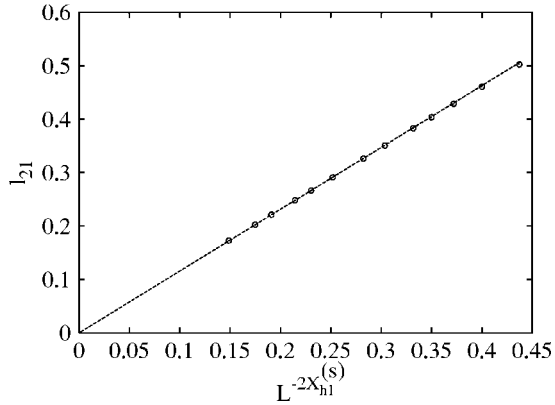

FIG. 6. Second moment l_{21} at the special transition $p_{1c}^{(s)} = 0.418\,17$, vs $L^{-2X_{h1}^{(s)}}$. The surface magnetic scaling dimensions $X_{h1}^{(s)} = 0.1986$ was taken from the fit.

TABLE I. Finite-size data of Q_1 and Q_b and their extrapolated values for $L\to\infty$. The bulk bond probability is $p_b=p_{bc}=0.248\,812\,6$ for columns 2–8. For the last column, one has $p_b=0$ and $p_1=1/2$, so that the system reduces to a two-dimensional bond-percolation model at criticality. For the ordinary, the special, and the extraordinary transitions, the surface probabilities were taken as $p_1=p_{bc}$, $p_1=p_{1c}^{(s)}=0.418\,17(2)$, and $p_1=0.54$, respectively.

	Ordinary		Special		Extraordinary		Periodic	
L	Q_1	Q_b	Q_1	Q_b	Q_1	Q_b	Q_b(3D)	Q_b(2D)
6	0.46304(3)	0.52890(6)	0.78145(3)	0.68183(5)	0.953774(6)	0.75379(3)	0.62994(5)	0.87331(2)
8	0.43405(3)	0.52590(6)	0.77388(3)	0.66255(5)	0.965311(5)	0.75293(3)	0.62868(5)	0.87158(2)
10	0.41688(3)	0.52473(6)	0.76982(3)	0.65962(5)	0.973709(4)	0.75305(3)	0.62836(5)	0.87082(2)
12	0.40565(3)	0.52425(6)	0.76740(3)	0.65792(5)	0.9797347(3)	0.75343(3)	0.62866(5)	0.87048(2)
14	0.39767(3)	0.52409(6)	0.76584(3)	0.65679(5)	0.984064(3)	0.75369(3)	0.62899(5)	0.87029(2)
16	0.39174(3)	0.52409(6)	0.76481(3)	0.65590(5)	0.987233(2)	0.75391(3)	0.62939(5)	0.87021(2)
20	0.38341(2)	0.52413(6)	0.76361(3)	0.65487(5)	0.991368(1)	0.75418(3)	0.63005(5)	0.87016(2)
24	0.37790(2)	0.52424(6)	0.76294(3)	0.65420(5)	0.993816(1)	0.75431(3)	0.63056(5)	0.87018(2)
28	0.37390(2)	0.52447(6)	0.76262(3)	0.65373(5)	0.995369(1)	0.75437(3)	0.63102(5)	0.87020(2)
32	0.37084(2)	0.52445(6)	0.76243(3)	0.65332(5)	0.996407(1)	0.75440(3)	0.63137(5)	0.87022(2)
40	0.36647(2)	0.52467(6)	0.76214(3)	0.65289(5)	0.997663(1)	0.75437(3)	0.63188(5)	0.87025(2)
48	0.36352(2)	0.52476(6)	0.76211(3)	0.65259(5)	0.998363(1)	0.75443(3)	0.63210(5)	0.87030(2)
64	0.35951(3)	0.52499(6)	0.76225(3)	0.65222(6)	0.999071(1)	0.75423(6)	0.63262(5)	0.87037(2)
80	0.35710(3)	0.52540(6)	0.76223(6)	0.65199(6)	0.999407(1)	0.75420(6)	0.63288(5)	0.87042(2)
120	0.35338(3)	0.52521(6)	0.76240(6)	0.65170(6)	0.999748(1)	0.75412(6)	0.63300(5)	0.87049(2)
∞	0.3414(4)	0.52555(7)	0.7629(2)	0.65130(8)	1	0.75390(8)	0.6338(2)	0.87053(2)

and c_{22}. These terms lead to a reduction of the residual χ^2 of the fits, but do not significantly modify the results. The surface thermal exponent was fixed at $y_{t1}^{(s)}=0.5387$ as found above. We obtain $p_{1c}^{(s)}=0.418\,16(4)$, $y_{h1}^{(s)}=1.8014(6)$, and $y_{i1}=-0.55(2)$. The quoted error margins include the uncertainty due to the error in $y_{t1}^{(s)}$. The estimate of the percolation threshold $p_{1c}^{(s)}$ is in agreement with that obtained from the fit of Q_1. The fit yields $b_2=-0.04(2)$, so that the term with b_2 is not very significant. The value of y_{i1} is mainly determined by the term with amplitude c_{21}. For clarity, the l_{21} data at $p_1=p_{1c}^{(s)}=0.418\,17(2)$ are shown in Fig. 6 versus $L^{2y_{h1}^{(s)}-4}$, where $y_{h1}^{(s)}=1.8015(6)$ as determined by the fit.

We also fitted Eq. (13) to the data of the pair correlation function g_{11}, and obtain $p_{1c}^{(s)}=0.418\,15(4)$, $y_{h1}^{(s)}=1.8016(6)$, and $y_{i1}=-0.54(2)$. These results are in agreement with those from Q_1 and l_{21}, and confirm the value of y_{i1}.

The present work also includes a determination of the asymptotic value of the bulk ratio Q_b. For this purpose, we performed additional simulations which included a decomposition of the whole lattice into clusters, at the estimated bulk percolation threshold $p_{1c}^{(s)}=0.418\,17(2)$. The system sizes were taken in the range $6\leqslant L\leqslant 120$. The Q_1 and Q_b data are shown in Table I. We fitted Q_b by

$$Q_b(L)=Q_{bc}^{(s)}+q_1L^{y_i}+q_2L^{y_{i1}^{(s)}}+q_3L^{-2}+q_4L^{-3}+q_5L^{-4}, \tag{14}$$

with the correction exponents y_i and $y_{i1}^{(s)}$ fixed at $-1.14(15)$ and -0.54, respectively. Just as for by the previous fit of Q_1, we did not find clear indications of the existence of a term with exponent y_{i1}. The fit yields $Q_{bc}^{(s)}=0.651\,30(8)$. The error margin may be somewhat larger if the correction exponents are different from our choice.

B. Ordinary transitions

We simulated at bulk criticality p_{bc} and took the surface bond-occupation probabilities as $p_1(z=1)=1$ and $p_1(z=L)=p_{bc}$, respectively. In other words, fixed boundary conditions were imposed on the surface $z=1$, so that all the lattice sites on this plane belong to the same cluster. As a consequence, we only formed a single cluster containing all sites at $z=1$, and we sampled the fraction l_{11} of the sites at $z=L$ in this cluster and the pair correlation function g_{11}. About 2.4×10^8 samples were taken for each of 15 system sizes in the range $4\leqslant L\leqslant 120$. The data for l_{11} and g_{11} are shown in Table II. They were fitted by

$$l_{11}(L)=L^{-X_{h1}^{(o)}}(a_0+a_1L^{y_i}+a_2L^{y_{i1}}+a_3L^{y_3}+a_4L^{y_4}) \tag{15}$$

and

$$g_{11}(L)=L^{-2X_{h1}^{(o)}}(b_0+b_1L^{y_i}+b_2L^{y_{i1}}+b_3L^{y_3}+b_4L^{y_4}), \tag{16}$$

where the terms with a_i and b_i $(i=1,2,3,4)$ account for finite-size corrections, and $X_{h1}^{(o)}=2-y_{h1}^{(o)}$ is the surface magnetic scaling dimension at the ordinary phase transition. We mention that the exponent in Eq. (15) is $X_{h1}^{(o)}$ instead of $2X_{h1}^{(o)}$ because of the fixed boundary conditions on the surface $z=1$. We took $y_i=-1.14(15)$ [28–30]. Since the surface ther-

TABLE II. Finite-size data of l_{11} and g_{11} for $p_b=p_{bc}=0.248\,81\,26(5)$, $p_1(z=1)=1$, and $p_1(z=L)=p_{bc}$.

L	4	6	8	10	12	16	20
l_{11}	0.24990(2)	0.17211(1)	0.13097(1)	0.105688(8)	0.088601(8)	0.067010(5)	0.053928(4)
g_{11}	0.12294(1)	0.060682(7)	0.035554(4)	0.023255(3)	0.016382(3)	0.009386(1)	0.006084(1)
L	24	28	32	40	64	80	120
l_{11}	0.045151(4)	0.038849(4)	0.034094(3)	0.027429(2)	0.017338(2)	0.013948(2)	0.009394(2)
g_{11}	0.0042647(7)	0.0031583(7)	0.0024329(2)	0.0015745(4)	0.0006290(1)	0.0004071(1)	0.0001846(1)

mal exponent is $y_{t1}^{(o)}=-1$, we set $y_2=-1$, $y_3=-2$, and $y4=-3$. However, the values of y_i and y_2 are so close to each other that only one of the terms with b_1 and b_2 was included in the fit. The analyses of l_{11} and g_{11} yield the surface magnetic scaling dimension as $X_{h1}^{(o)}=0.9754(4)$ and 0.9753(4), respectively, where the error margins are again quoted as two standard deviations. These estimates are in good agreement with each other, and further improve the existing results $X_{h1}^{(o)}=0.970(6)$ [21] and $X_{h1}^{(o)}=0.976(4)$ [9]. An illustration of the quality of these fits is provided in Fig. 7, where the l_{11} data are shown versus $L^{-X_{h1}^{(o)}}$ with $X_{h1}^{(o)}=0.9754$.

To determine the universal values $Q_{1c}^{(o)}$ and $Q_{bc}^{(o)}$, we performed simulations at $p_b=p_{bc}=0.248\,812\,6(5)$ [28] and $p_1(z=1)=p_1(z=L)=p_{bc}$; the whole lattice was decomposed into clusters. As one can see in Fig. 3, this point is rather close to the fixed point $p_{1c}^{(o)}$ for the ordinary transition, and thus one does not expect serious crossover phenomena from the special transition. The system sizes were taken in the range $6\leqslant L\leqslant 120$. The finite-size data of the surface ratio Q_1 are shown versus $L^{-0.65}$ in Fig. 8, which indicates that slowly convergent corrections are indeed induced by the open surfaces. According to the least-squares criterion, we fitted the Q_1 data by

$$Q_1(L)=Q_{1c}^{(o)}+b_1L^{y_{i1}}+b_2L^{y_i}+b_3L^{-2}+b_4L^{-3}+b_5L^{-4}, \tag{17}$$

where the exponent y_i was fixed at $-1.14(15)$. First, we excluded the term with b_2, and obtain $Q_{1c}^{(o)}=0.3414(4)$ and $y_{i1}=-0.64(2)$. The result y_{i1} does not seem to be in agreement with the exact value $y_{t1}^{(o)}=-1$. This may suggest that, apart from those with exponent -1, additional slowly decaying corrections can exist at the ordinary transition. When the term with b_2 was included, the fit of Q_1 yields $yi1=-0.62(10)$. We also fitted the Q_b data by Eq. (17), and obtain $Q_{bc}^{(o)}=0.525\,55(7)$. For clarity, the Q_1 and Q_b data are shown in Table I.

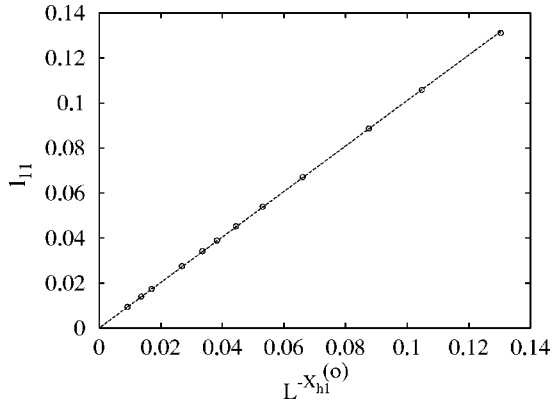

FIG. 7. Surface quantity l_{11} at the ordinary transition with $p_1(z=1)=1$ and $p_1(z=L)=p_{bc}$ vs $L^{-X_{h1}^{(o)}}$. The value $X_{h1}^{(o)}=0.9754$ was taken from the fit.

C. Extraordinary transition

At the extraordinary phase transition $p_b=p_{bc}$, $p_1>p_{1c}^{(s)}$, the largest cluster occupies a finite fraction of the surfaces, so that, for $L\to\infty$, the surface ratio Q_1 is equal to 1 and the correlation functions g_{11} and g_{12} approach nonzero constants. However, since the bulk maintains long-ranged critical correlations, the surfaces can also display some "critical" behavior. This is indicated by the clean intersection of the Q_b data near $p_{1c}^{(e)}\approx 0.54$, which is shown in Figs. 3 and 9.

Thus, more extensive simulations were performed at bulk criticality p_{bc} with $p_1=0.54$, in order to sample the surface correlation function g_{12} with an adequate statistical accuracy. The system size L took 15 values in the range $6\leqslant L\leqslant 120$, and for each system size, a number of about 2×10^8 samples was taken. Part of the g_{12} data are shown in Fig. 10. As expected, these figures confirm that (1) in the thermodynamic limit $L\to\infty$, l_{21} and g_{12} assume nonzero values, and (2) the decay of these quantities with L obeys a power law, as expected for correlation functions at criticality. We fitted the g_{12} data by

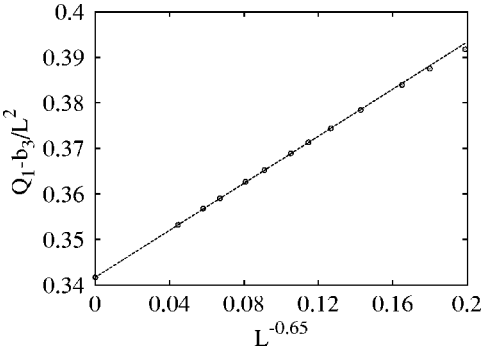

FIG. 8. Surface ratio Q_1 at the ordinary transition with $p_1(z=1)=p_1(z=L)=p_{bc}$, shown as Q_1-b_3/L^2 vs $L^{y_{i1}}$. The values $Q_1(L\to\infty)=0.3414$, $b_3=2.1$, $y_{i1}=-0.64$ were taken from the fit.

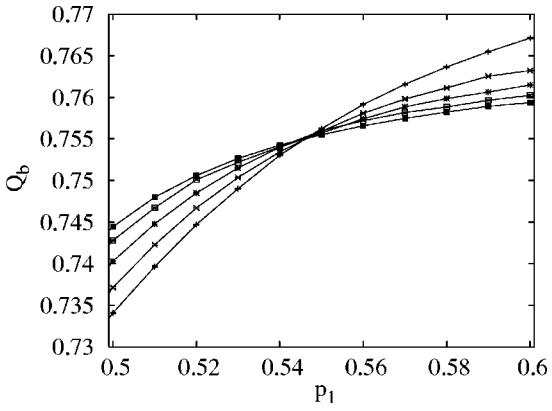

FIG. 9. Bulk ratio Q_b at the extraordinary transition in the range $0.5 \leqslant p_1 \leqslant 0.6$. The data points +, □, ○, △, and ◇ represent system sizes $L=8$, 12, 16, 20, and 24, respectively.

$$g_{12}(L) = g_a + L^{-X_{h1}^{(e)}}(g_0 + g_1 L^{y_i} + g_2 L^{y_2} + g_3 L^{y_3} + g_4 L^{y_4}). \tag{18}$$

We mention that the exponent in Eq. (18) is $X_{h1}^{(e)}$ instead of $2X_{h1}^{(e)}$, because the nonzero background g_q leads to behavior of the quantity g_{12} as a one-point correlation function. We took the correction exponents as $y_i=-1.14(15)$, $y_2=-2$, $y_3=-3$, and $y_4=-4$. We obtain $g_a=0.4747(6)$ and $X_{h1}^{(e)}=0.75(6)$.

The data of the ratios Q_1 and Q_b are shown in Table I. They were fitted by Eq. (17). We obtain $Q_{1c}^{(e)}=0.999\,98(2)\approx 1$ and $Q_{bc}^{(e)}=0.753\,90(8)$.

D. Surface transition

For the bulk bond probability $p_b < p_{bc}$, a line $p_{1c}(p_b)$ of phase transitions, in the two-dimensional percolation universality class, exists on the surfaces. In particular, for $p_b=0$ the system reduces to the bond-percolation model on the square lattice, for which the percolation threshold lies exactly at $p_{1c}(p_b=0)=1/2$.

In this subsection we aim to numerically locate the critical line $p_{1c}(p_b)$ by analyzing the Q_1 data. Since the asymptotic value of Q_1 is universal, we first simulated the square-lattice bond-percolation model at $p_{1c}(p_b=0)=1/2$. The system sizes were taken in the range $6 \leqslant L \leqslant 120$. The Q_1 data, shown in Table 1, were fitted by

$$Q_1(L) = Q_{1c} + b_1 L^{y_i} + b_2 L^{y_a} + b_3 L^{-3} + b_4 L^{-4}, \tag{19}$$

where $y_i=-2$ is the exponent of the leading irrelevant field. The term with b_2 arises from the background, and the exponent y_a is obtained as $y_a=2-2y_h^{(d=2)}=-43/24$, where $y_h=91/48$ [26] is the magnetic exponent of the percolation model in two dimensions. It was recently reported [33] that, in principle, the term with b_1 should be replaced by $b_1 \ln(L/L_0)/L^2$, where L_0 is an unknown constant. However, such a logarithmic factor is difficult to observe numerically in a correction term, and it hardly influences the results of the fit. Thus, we still used Eq. (19) to fit Q_1 data, and obtain the universal value $Q_{1c}=0.870\,53(2)$.

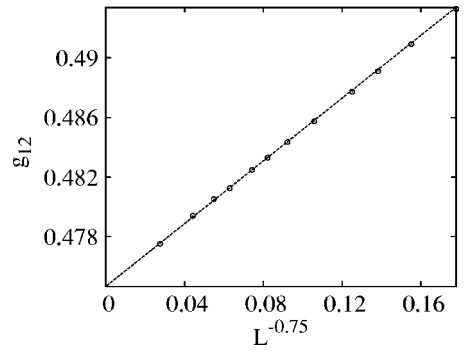

FIG. 10. Surface correlation function g_{12} at the extraordinary phase transition with $p_1=0.54$ vs $L^{-0.75}$.

Next, we performed simulations of the three-dimensional bond-percolation model at bulk probabilities $p_b=0.1$, 0.15, 0.18, 0.20, 0.22, 0.23, 0.24, 0.244, and 0.247. For each value of p_b, the percolation threshold $p_{1c}(p_b)$ was first roughly estimated from the Q_1 data. Then, longer simulations of about 10^8 steps were carried out near $p_{1c}(p_b)$, for 12 system sizes in the range $6 \leqslant L \leqslant 120$. The Q_1 data were fitted by

$$\begin{aligned} Q_1(p_1,L) = Q_{1c} + \sum_{k=1}^{4} a_k (p_1 - p_{1c})^k L^{k y_t^{(d=2)}} + b_1 L^{-2} + b_2 L^{-3} \\ + b_3 L^{-4} + n(p_1 - p_{1c})^2 L^{y_t^{(d=2)}} + r_0 L^{y_a} r_1 (p_1 \\ - p_{1c}) L^{y_a} + r_2 (p_1 - p_{1c})^2 L^{y_a}, \end{aligned} \tag{20}$$

where $y_t^{(d=2)}=3/4$ is the thermal exponent of the two-dimensional percolation model. The exponent y_a was taken as $2-2y_h^{(d=2)}=-43/24$, and the universal value of Q_{1c} was fixed at 0.870 53(2). The results are shown in Table III, where the quoted error margins include the uncertainty of Q_{1c}.

IV. DISCUSSION

We have determined the surface bond-occupation probability of the bond-percolation model on the simple-cubic

TABLE III. Results for the surface phase transition and the special transition; the latter are labeled by the asterisk.

p_b	0	0.1	0.15	0.18	0.2	0.22
p_{1c}	1/2	0.49915(6)	0.49605(6)	0.49151(6)	0.48603(6)	0.47657(6)
p_b	0.23	0.24	0.244	0.247	0.2488126(5)*	
p_{1c}	0.46883(6)	0.45655(6)	0.44832(6)	0.4326(4)	0.41817(2)*	

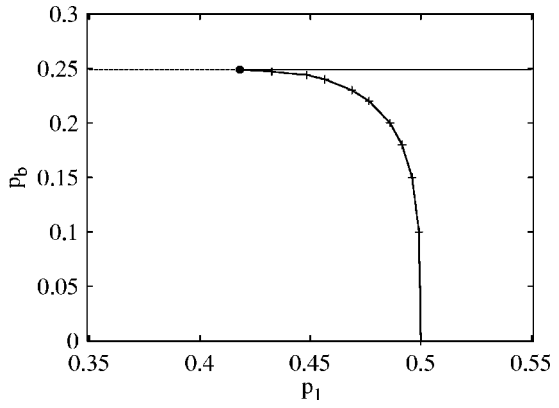

FIG. 11. Phase diagram for the bond-percolation model on the simple-cubic lattice with free surfaces in one direction. Dashed line: ordinary transition. Thin full line: extraordinary transition. Thick curve: surface transition. The special transition is shown as ●.

lattice at the special transition as $p_{1c}^{(s)}=0.4187(2)$, and we have located the line of surface transitions $p_{1c}(p_b)$. On the basis of these numerical results, the phase diagram is shown in Fig. 11. We have also obtained the universal values of the surface critical exponents as $y_{h1}^{(o)}=1.0246(4)$, $y_{t1}^{(s)}=0.5387(2)$ and $y_{t1}^{(s)}=1.8014(6)$, and $y_{h1}^{(e)}=1.09(3)$ for the ordinary, the special, and the extraordinary phase transition, respectively. Near the special transition $(p_{bc},p_{1c}^{(s)})$, the line of the surface transition can be asymptotically described as $(p_b-p_{bc}) \propto (p_{1c}-p_{1c}^{(s)})^{1/\Psi}$, where the crossover exponent is $\Psi=y_{t1}^{(s)}/y_t =0.465(12)$. The error margin of Ψ is mainly due to the uncertainty of the bulk thermal exponent $y_t=1.141(5)$.

Again, we find that dimensionless ratios like Q_1 and Q_b in Eq. (7) are very useful in Monte Carlo determinations of critical points. At criticality, the asymptotic values of Q_1 and Q_b are universal, although they depend on the boundary conditions. We have also simulated the bond-percolation model on the simple-cubic lattice with periodic boundary conditions in the range $6 \leqslant L \leqslant 120$. The Q_b data at $p_b=p_{bc}=0.248\,821\,6(5)$ [28] are shown in Table I. These data were fitted by Eq. (17), which leads to $Q_{bc}(d=3)=0.6338(2)$.

The existence of the aforementioned extraordinary transition, and in particular that of the line of surface transitions, is related to the fact that the two-dimensional surfaces can sustain long-range order in the absence of an ordered bulk. But even without spontaneous surface order, rich surface critical phenomena can still occur. For instance, for the Heisenberg model in three dimensions, the line of surface transitions does not exist, and only the ordinary transition occurs on the surfaces. Nevertheless, at bulk criticality $K=K_c$ and for surface couplings $K_1/K \geqslant 2.0$, it was reported [34] that spurious long-range order occurs on the surfaces and the surface magnetic exponent becomes K_1/K dependent. Another remarkable example is the two-dimensional Potts model at its tricritical point K_t, where the surfaces are just one-dimensional edges. Although the surface transition occurring at $K<K_t$ does not exist on the edges, various types of edge phase transition have been found [35–37] when the surface coupling and/or the surface field is varied. In particular, spontaneous one-dimensional order occurs on the edges when the surface coupling is moderately enhanced.

ACKNOWLEDGMENTS

The authors are indebted to Jouke Heringa, Xiaofeng Qian, and Bob Ziff for valuable discussions. This research was supported by the Dutch FOM foundation ("Stichting voor Fundamenteel Onderzoek der Materie") which is financially supported by the NWO ("Nederlandse Organisatie voor Wetenschappelijk Onderzoek")

[1] K. Binder, in *Phase Transitions and Critical Phenomena*, edited by C. Domb and J. L. Lebowitz (Academic Press, London, 1987), Vol. 8, p. 1, and references therein.
[2] H. W. Diehl, in *Phase Transitions and Critical Phenomena* (Ref. [13]), Vol. 10, p. 76, and references therein.
[3] J. L. Cardy, in *Phase Transitions and Critical Phenomena* (Ref. [13]), Vol. 11, p. 55, and references therein.
[4] D. P. Landau and K. Binder, Phys. Rev. B **41**, 4633 (1990), and references therein.
[5] C. Ruge and F. Wagner, Phys. Rev. B **52**, 4209 (1995).
[6] M. P. Nightingale and H. W. J. Blöte, Phys. Rev. B **48**, 13678 (1993).
[7] K. Binder, D. P. Landau, and M. Muller, J. Stat. Phys. **110**, 1411 (2003).
[8] H. W. Diehl, Int. J. Mod. Phys. B **11**, 3503 (1997).
[9] Y. Deng and H. W. J. Blöte, Phys. Rev. E **67**, 066116 (2003); **69**, 066129 (2004).
[10] M. Pleimling, J. Phys. A **37**, R79 (2004).
[11] M. Pleimling and W. Selke, Eur. Phys. J. B **1**, 385 (1998).
[12] L. Onsager, Phys. Rev. **65**, 117 (1944).
[13] Y. Deng and H. W. J. Blöte, Phys. Rev. E **68**, 036125 (2003), and references therein.
[14] T. C. Lubensky and M. H. Rubin, Phys. Rev. B **12**, 3885 (1975).
[15] T. W. Burkhardt and J. L. Cardy, J. Phys. A **20**, L233 (1987).
[16] C. Ruge, S. Dunkelmann, and F. Wagner, Phys. Rev. Lett. **69**, 2465 (1992).
[17] J. M. Kosterlitz and D. J. Thouless, J. Phys. C **5**, L124 (1973).
[18] D. P. Landau, R. Pandey, and K. Binder, Phys. Rev. B **39**, 12302 (1989).
[19] K. De'Bell and J. W. Essam, J. Phys. A **14**, 1993 (1981).
[20] A. Hansen, P. M. Lam, and S. Roux, J. Phys. A **22**, 2635 (1989).
[21] P. Grassberger, J. Phys. A **25**, 5867 (1992).
[22] S. R. Broadbent and J. M. Hammersley, Proc. Cambridge Philos. Soc. **53**, 629 (1957).
[23] D. Stauffer and A. Aharony, *Introduction to Percolation Theory* (Taylor and Francis, London, 1992), and references therein.
[24] M. Sahimi, *Applications of Percolation Theory* (Taylor and Francis, London, 1994).

[25] D. C. Mattis, *Statistical Mechanics Made Simple* (World Scientific, Singapore, 2003).
[26] See, e.g., F. Y. Wu, Rev. Mod. Phys. **54**, 235 (1982).
[27] P. W. Kasteleyn and C. M. Fortuin, J. Phys. Soc. Jpn. **26** (Suppl.), 11 (1969).
[28] C. D. Lorenz and R. M. Ziff, Phys. Rev. E **57**, 230 (1997).
[29] G. Paul, R. M. Ziff, and H. E. Stanley, Phys. Rev. E **64**, 026115 (2001).
[30] C. K. Hu, J. A. Chen, N. S. Izmailian, and P. Kleban, Comput. Phys. Commun. **126**, 77 (2000).
[31] R. H. Swendsen and J.-S. Wang, Phys. Rev. Lett. **58**, 86 (1987).
[32] K. Binder, Z. Phys. B: Condens. Matter **43**, 119 (1981).
[33] J. L. Cardy, e-print cond-mat/0111031.
[34] M. Krech, Phys. Rev. B **62**, 6360 (2000).
[35] L. Chim, Int. J. Mod. Phys. A **11**, 4491 (1996).
[36] I. Affleck, J. Phys. A **33**, 6473 (2000).
[37] Y. Deng and H. W. J. Blöte, Phys. Rev. E **70**, 035107 (2004).